



# Single fiber swelling behavior for natural and man-made cellulose fibers under alkaline treatment

Xiang You · Feng Chen · Yibo Ma · Annariikka Roselli · Eric Enqvist · Heikki Hassi

Received: 6 July 2021 / Accepted: 19 October 2021 / Published online: 30 October 2021  
© The Author(s), under exclusive licence to Springer Nature B.V. 2021

**Abstract** Swelling behavior of cotton, dissolving wood pulp (DWP), viscose staple fiber, and Tencel staple fiber in varying sodium hydroxide (NaOH) concentration were investigated by means of optical microscopy and were characterized by molecular mass distribution, X-ray diffractometer, and dynamic vapor sorption. The effect of temperature (20–45 °C) and duration (0–120 min) was studied. The results reveal that the swelling ratio of fiber in alkali solution depends on fiber accessibility and NaOH concentration. Viscose staple fiber exhibited the highest swelling ratio and lowest swelling ratio observed for

dissolving wood pulp fiber among all the materials. The cotton or DWP fibers provide maximum swelling during alkaline steeping (18wt % lye) at higher temperatures, i.e., 45 °C. As for viscose staple fiber and Tencel staple fiber, using 12 wt% lye concentration and steeping at lower temperatures, i.e., 20 °C maximum swelling behavior.

**Keywords** Swelling · Cotton · Dissolving wood pulp · Regenerated cellulose · Cell wall

**Supplementary Information** The online version contains supplementary material available at <https://doi.org/10.1007/s10570-021-04280-0>.

X. You (✉) · A. Roselli · E. Enqvist · H. Hassi (✉)  
Scitech-Service Oy, 00130 Helsinki, Finland  
e-mail: xiang.you@scitech.fi

H. Hassi  
e-mail: heikki.hassi@scitech.fi

F. Chen · Y. Ma  
Department of Bioproducts and Biosystems, School of Chemical Engineering, Aalto University, 00076 Aalto, Finland

F. Chen  
Wood Materials Science Group, Institute for Building Materials, ETH Zurich, 8093 Zurich, Switzerland

A. Roselli  
Metsä Spring Oy, 02150 Espoo, Finland

## Introduction

Cellulose, an almost inexhaustible renewable biodegradable source, is considered a promising raw material for producing bio-based products that have the potential to reduce marine pollution and plastic waste (Klemm et al. 2005). Cellulose is relatively stable due to the high degree of crystallization and strong inter- and intramolecular hydrogen bonds (Henigues et al. 2011). The hydrophobic interactions between the cellulose molecular sheets in the crystallite also restrict the dissolution of cellulose (O'Sullivan 1997, Nishiyama et al. 2002, 2003, Foress and Fremer 2003). Only a few solvents can directly dissolve cellulose (Gross and Chu 2010). The direct cellulose solvents can be classified into the system: aqueous media and non-aqueous media. Aqueous media consists of aqueous inorganic complexes,

aqueous alkaline (NaOH), acids, and molten inorganic salt hydrates. Non-aqueous media includes ionic liquids (ILs), organic solvent, dimethyl sulfoxide, and amine oxide monohydrate (NMMO) (Heinze and Koschella 2005; Liebert 2010; Sen and Martin 2013, Olsson and Westman 2013). Of all direct solvents, only NMMO monohydrate is used as a direct cellulose solvent on an industrial scale for spinning textile fibers (Lyocell process) (Chen et al. 2020).

The dissolution mechanisms of cellulose fibers in various direct solvents have been studied in detail. When native cotton and wood fibers are placed in a particular swelling or dissolution agent, they show nonhomogeneous swelling. The solvent first penetrates the Primary (P) cell wall through pores and dissolves the cellulose in the Secondary (S) cell wall. Since the cellulose chains are still trapped inside the fiber structure, and the solvent penetration continues, due to osmotic pressure, the increasing solvent volume causes the expansion of the P cell wall (ballooning) (Cuissinat and Navard 2006, Le Moigne et al. 2010, Olsson et al. 2014, Mäkelä et al. 2018). According to the study of Cuissinat and Navard (2006), the behavior of dissolving wood pulp (DWP) or cotton fibers in various solvent systems (for example, NaOH-water or NMMO with 25 to 35% water) can be characterized by five particular modes: Mode (1) Accelerated dissolution by disintegration into cellulose fragments. Mode (2) Swelling in a large area by ballooning followed by dissolution. Mode (3) Large swelling by ballooning, but without dissolution. Mode (4) Homogeneous swelling without dissolution. Mode (5) No swelling and no dissolution. These modes reflect the quality of the solvents from excellent, moderate, weak, and non-solvent. In less powerful solvents, ballooning may be followed by bursting of S1 and then dissolution (Cuissinat and Navard 2006, Kihlman et al. 2012, 2013, Zhang et al. 2013, Mäkelä et al. 2018, Chen et al. 2020). For DWP fibers, the swelling of S2 layer of the S wall begins from the lumen (i.e., filled with NaOH solution). The ballooning occurs and generates tension to fibrils of P wall and S1 layer, which are less prone to swelling due to their more random fibril orientation (Cuissinat and Navard 2006, Zhang et al. 2013). This tension further hinders the swelling of P and S1, P wall bursts and forms collars that remain undissolved, which locally prevent swelling of S wall (Cuissinat and Navard 2006, Zhang et al. 2013). Finally, also S1 layer bursts and gets

fragmented, then dissolved in the form of aggregates. The exact mechanisms apply to cotton fibers. However, cotton is considered more challenging to swell than wood pulp, which could be explained by the many sub-layers in its cell wall structure, with different orientation directions (Klemm et al. 2005).

The microfibrillar structure of a man-made cellulosic fiber strongly resembles the original fibrillar structure of DWP cell wall layers. To understand fiber swelling and dissolution behavior various factors must be taken into account: their chemical composition, properties of primary and secondary layers in natural fibers or properties of skin in some man-made fibers, porosity, cellulose crystallinity, and molecular weight (Abu-Rous et al. 2006). Currently, approximately 7.1 million mt per annum (Preferred fiber & materials market report 2020) of man-made cellulosic fiber (MMCFs) is manufactured globally. The viscose process is still by far the dominating process used in the fiber industry. At the same time, the recent promotion of the circular economy in the textile industry encouraged the utilization of waste cotton products as a novel source for viscose grade dissolving pulp. The viscose process is a well-established technology with an industrial history of over 100 years. However, the viscose process also presents specific weaknesses, i.e., high investment cost, long throughput time, and challenging process control. The common rationale behind these weaknesses is the inherently problematic processability of the fibers dissolving wood pulp in the multi-step chemical conversion during the viscose process. Furthermore, dissolving pulp made of recycled cotton textiles brings new challenges to viscose manufacturers and the textile industry.

Under conditions close to the steeping step of the industrial viscose process, the swelling behavior of cotton, dissolving wood pulp, and man-made fibers is an idle research field. It is essential to conduct fundamental studies which may contribute to understanding the cellulose swelling behaviors and further work on developing the viscose process. This paper studies the swelling ratio and morphological changes of the structures of the single fiber in different NaOH solution concentrations and temperatures. The fibers' swelling behavior is observed by using optical microscopy.

## Experimental methods

### Materials

Raw cotton fiber without seed was obtained from Zhengzhou Share Machinery Co., Ltd, China. A commercially available DWP sheet was obtained from Domsjö, Sweden. The Domsjö DWP was made from softwood chips (spruce/pine 60:40) collected from local sawmills and cooked by Domsjö sulfite pulping process. Two other man-made fibers VsF (1.3 dtex, 39 mm, bright, raw-white) and TsF (1.3 dtex, 38 mm, bright, raw-white), were donated by Lenzing, Austria. The characteristics of the fibers are presented in Table 1. The solution was prepared by dissolving solid NaOH pallet in the milli-Q water to 5.5, 12, and 18% NaOH concentrations. All concentrations ratios are presented as % by weight (wt). All materials were cut into shorter lengths (fiber length  $\leq 5$  mm) before the test.

### Method

#### *Molecular mass distribution (MMD) of cellulose fibers*

MMD of the raw materials was determined by gel permeation chromatography. About 500 mg of the fiber sample was accurately weighed into a sample bottle. The samples were activated by a water–acetone–N,N-dimethylacetamide (DMAc) sequence. The activated samples (50 mg each) were dissolved in 90 g L<sup>-1</sup> lithium chloride containing DMAc at room temperature and under gentle stirring (Schelosky et al. 1999). The samples were then diluted to 9 g L<sup>-1</sup> LiCl/DMAc, filtered with 0.2  $\mu$ m syringe filters, and analyzed in a Dionex Ultimate 3000 system with a guard column, four analytical columns (PLgel Mixed-A, 7.5  $\times$  300 mm) and refractive index (RI) detection (Shodex RI-101). Flow rate and temperature were 0.75 mL min<sup>-1</sup> and 25 °C, respectively. Narrow pululan standards (343–2,500 kDa, PSS GmbH) were

used to calibrate the system. Number-average and weight-average molar mass,  $M_n$  and  $M_w$ , were calculated.

#### *Determination of the crystallinity index with X-ray diffractometer*

X-ray diffraction (XRD) data of the precursor fiber were collected in the transmission mode setting of Cu-K $\alpha$  X-ray instrument, SmartLab (RIGAKU) operated at 45 kV and 200 mA. Cellulose fiber was ground using Wiley mill having 60  $\mu$ m mesh size. The samples were then pressed into disks using a pellet press instrument for 30 s. Powder diffraction data were collected in a continuous mode from 5° to 60° 2 $\theta$  by  $\theta/2\theta$  scan setting. Scattering profiles were corrected for smoothing, subtracting air scattering, and subtracting inelastic contribution. The amorphous cellulose contribution was subtracted from remained elastic scattering profile using a smoothing procedure as previously described (Guizani et al. 2020) applying Savitzky-Golay filter from 8° to 55° 2 $\theta$  for each diffraction profile. Window size and polynomial order for the Savitzky-Golay filter were set to 201 (corresponding to 4° by 2 $\theta$ ) and 1, respectively. Iteration for the background estimation was repeated until the iteration did not reduce the background area significantly. The figures of the smoothed original XRD spectrum and subtracted spectrum are shown in Figure S1. In this experimental and smoothing condition, the smoothing procedure was repeated 50 times. Thus, estimated amorphous contribution ( $I_{bkg}(2\theta)$ ) is used as a background profile to estimate the crystallinity index ( $CI$ ) from 9° to 50° 2 $\theta$ :

$$CI(\%) = 100 \times \left( \frac{\int I(2\theta)d2\theta - \int I_{bkg}(2\theta)d2\theta}{\int I(2\theta)d2\theta} \right) \quad (1)$$

**Table 1** Characteristics of cellulose fibers

Sample	$M_n$ (kDa)	$M_w$ (kDa)	$CI$ (%)	$M_s$ (%)	$t_s$ (min)	$t_{des}$ (min)
Raw cotton	324	444	49.8	12.7	1113	1170
DWP	59	208	45.8	13.8	1260	1220
VsF	26	57	32.2	21.8	1675	2243
TsF	40	127	39	18.9	1497	1885

### Dynamic vapor sorption (DVS)

The extent of moisture sorption is defined as fiber accessibility (Okubayashi et al. 2004). A DVS intrinsic apparatus (Surface Measurement system, London, UK) measuring accuracy of 0.1  $\mu\text{g}$  was used for water vapor sorption analysis. Around 10 mg of pre-dried ground fibers were placed in the sample pan and preconditioned at a relative humidity (RH) of 0% at 25 °C until the equilibrium was reached using nitrogen (flow rate 100  $\text{cm}^3 \text{s}^{-1}$ ). The adsorption cycle was performed in 0% RH steps to a maximum of 90% RH, and vice versa for the desorption cycle. In both cases, the RH was kept constant until a defined equilibrium condition was reached, for example, when sample mass change was below 0.001% per minute over 10 min. Then RH was increased to 90%, and sample weight evolution and time to reach equilibrium ( $t_s$ ) were recorded. The RH was decreased to 0% for desorption, and time to reach equilibrium ( $t_{des}$ ) was recorded. Moisture sorption  $M_s$  (from  $M_0$  to  $M_{90}$  at 90% RH) were calculated as follows:

$$M_s = \frac{M_{90} - M_0}{M_0} \times 100\% \quad (2)$$

### Optical microscopy observations of fiber swelling

The single fiber was placed between two glass plates with the in-between distance of around 140  $\mu\text{m}$  controlled by spacers. The distance between two glass slides is much larger than the fiber's thickness. The ends of the fiber were fixed by tape, and 1–2 drops of solvents were added. A Zeiss Axio optical microscope recorded fiber width in transmission mode equipped with a CCD camera (Metallux 3, Leitz) and Linkam TMS 91 hot stage to control temperature. The evolution of the fiber width in time  $t$  was calculated as  $D_t/D_0$ , where  $D_0$  and  $D_t$  are the initial width of the fiber at  $t = 0$  and the fiber width at time  $t$ , respectively. The experiment methods were performed similarly according to Chen et al. (2020)

## Results and discussion

### Physico-chemical properties of cellulose fibers

Cotton is a natural cellulose fiber (cellulose content  $\sim 99\%$ ) with a complex morphology; its elementary fiber consists of more secondary (S) cell wall layers than wood fiber. The sub-layers of S wall are highly ordered and have a compact structure with the microfibril lying parallel to one another (Cuissinat and Navard 2006).

The wood chips for Domsjö DWP production were the by-product from Sweden sawmills, from the outer part of the wood logs. These wood chips from sawmills mainly consisted of sapwood. This study does not focus on the difference in the wood chips comprised of a mixture of sapwood and heartwood. Deslauriers et al. (2006) reported that sulfite pulps are more suitable for exceptional paper grades, tissue, and dissolving pulp. DWP has special properties, including high  $\alpha$ -cellulose content ( $>90\%$  of dry matter), low hemicellulose content ( $<5\%$  of dry matter), virtually complete removal of lignin, and relatively low molecular weight than cotton fiber (Sixta 2006, Mozdyniewicz et al. 2013).

VsF is made via xanthation of alkali cellulose made of DWP, followed by dissolution and regeneration of the fibers by wet spinning in an acidic coagulation bath. Viscose fiber has folded perimeter and a skin–core structure due to immediate solidification of the outermost fiber surface. There is an adequately oriented skin layer and poorly oriented core, i.e., due to the non-Newtonian flow of viscose dope through spinneret orifices (Abu-Rous et al. 2006). TsF is made via direct dissolution in NMMO and spinning using the Lyocell process. TsF has a more oriented fiber structure because of the slower solvent exchange between the fiber and the coagulation media. TsF consists of semipermeable skin, porous middle zone, and dense fibre core (Schuster et al. 2003, Abu-Rous et al. 2006, 2007). And this structure is demonstrated by Chaudemanche and Navard (2011), that TsF skin is much less crystalline than the core.

To better understand the swelling behavior of the selected materials, a few physical properties need to be characterized. The number-average ( $M_n$ ) and weight-average ( $M_w$ ) molecular weights of cellulose in each fiber are presented in Table 1, and the corresponding

molar mass distribution is demonstrated in Fig. 1a. The MMD of the raw cotton shows a narrow distribution, which is according to what others have found for native cotton fibers (Timpa and Ramey 1989, Kleman-Leyer et al. 1992, Palme et al. 2014). Unlike cotton, the DWP sample revealed subtle shoulder and high molecular weight peaks indicating the presence of both low molar mass hemicellulose and relative long-chain cellulose. A distinct low molecular weight peaks for VsF and TsF are similar for all man-made fibers. It has to be noticed that cotton and VsF needed more time (2 weeks) to completely dissolve in LiCl/DMAc solution before the chromatographic analysis. The reason for cotton is its high

molecular weight, and the possible reason for VsF is the low accessibility caused by hornification. Moreover, the crystallinity of the material governs their swelling behavior.

The XRD patterns for the fibers are shown in Fig. 1b. Cotton cellulose spectrum accordingly represents Cell-I, containing both crystalline and amorphous regions. Its Cell-I has a crystallinity index of approximately 49.8%, typical for plant cellulose (Placet et al. 2012, Moryganov et al. 2018, Chen et al. 2020). DWP has a slightly lower crystallinity than cotton due to intensive pulping procedures and a small amount of amorphous hemicellulose. The MMCFs demonstrate the Cell-II allomorph, as expected. The *CI* is around 32.2% and 39% for VsF and TsF, respectively (Table 1). These results are in agreement with the previously reported crystallinity of MMCFs (Kreze and Malej 2003).

The dynamic water vapor sorption and desorption were measured to compare the accessibility of the fibres. Moisture sorption ( $M_s$ ), time to reach equilibrium  $t_s$  from 0 to 90% RH, and time to get equilibrium  $t_{des}$  from 90 to 0% RH for each fiber are shown in Table 1. Cotton absorbs the least vapor, probably because of the ‘resistant’ primary wall (Okubayashi et al. 2004; Xie et al. 2011) and higher cellulose crystallinity (*CI* 49.8%). In the study of Abu-Rous et al. (2006), cotton showed tiny pores in the bulk of the fiber, but the drying cracks and flat pores between the sheets of the secondary wall appear as larger pores. Similar to the cotton fiber, the DWP also demonstrates relatively low vapor sorption due to the high crystallinity (*CI* 45.8%). The DWP showed a stronger meridian scattering (004) at  $2\theta$  34° than cotton. This indicates a difference in the preferred orientation of the DWP and cotton samples. The different orientation of fiber-axis direction can be expected for the DWP sample in the powder pellet. This possibly affect the crystallinity calculation. Nevertheless, the *CI* calculated from Segal method (Table S1) demonstrated the same trend for cotton and DWP *CI* extrapolated with the current method. VsF absorbs the highest amount of moisture ( $M_s$ ) due to its lowest crystallinity (*CI* 32.2%) and wide pore size distribution from nanometre to micrometer scale (Okubayashi et al. 2005, Abu-Rous et al. 2006). Time to reach equilibrium,  $t_s = 1260$  min, is the longest for VsF among the selected fibers. It probably could be explained by the hornification phenomena (Siroka et al. 2008) as viscose fibers may

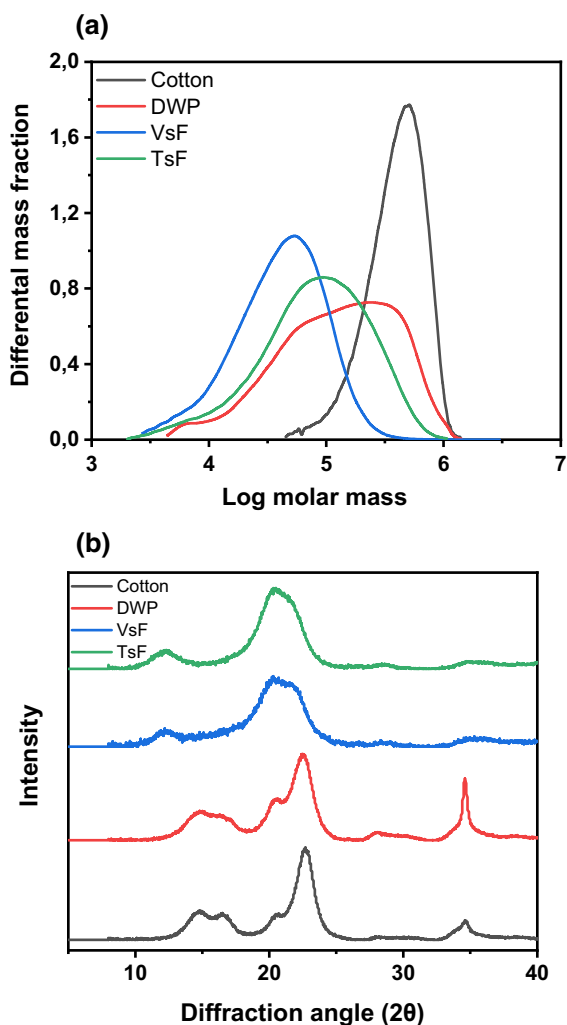


**Fig. 1** (a) Molecular mass distributions (MMD) and (b) X-ray diffraction (XRD) profiles of cotton, DWP, VsF and TsF

be overdried. The absorption of a larger amount of vapor takes more time, related to its large surface area. TsF contains only nanopores in the bulk of the fiber with a slight gradient in pore density and a very porous outer layer. As a result, TsF shows slightly lower moisture sorption than VsF. Cotton appears to absorb only a little water; Tencel shows uniform water absorption over the whole fiber cross-section, and uneven water distribution can be found in viscose fiber (Abu-Rous et al. 2006).

#### Fiber swelling behavior in NaOH solution

During the observation, the ends of the single fiber were fixed by tape for better monitoring by an optical microscope, and then the solvent was added. The fibers swelling is inwards in these fundamental studies. With one end fixed and with both ends free, it does not affect the swelling mechanism, only slightly affects swelling and dissolving rate (Chen et al. 2020).

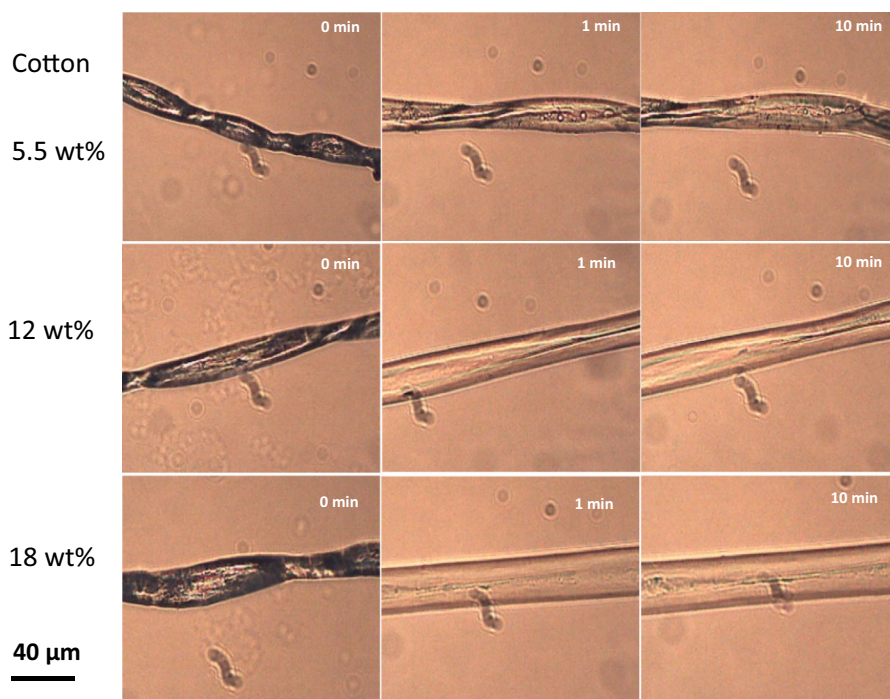
#### Cotton

As shown in Fig. 2, dried cotton fiber collapses into a flattened bean-like cross-section. It also twists along

its length to look like a twisted and flattened ribbon (Fig. 2, 0 min). These twists are called convolutions: about 60 convolutions per centimeter (Dochia et al. 2012). In this study, the width of convolutions was measured to indicate the cotton fiber swelling ratio evolution. The treatment temperature of 36 °C and 45 °C were chosen because they are close to the process conditions in the viscose process. A higher concentration is necessary for the viscose process to ensure that the conversion to the alkoxide derivative proceeds to an acceptable extent. Thus, in the industrial viscose process, the typical NaOH concentration is around 17–19 wt%, and conditions are generally performed at 30–55 °C. (Cuissinat and Navard 2008, Wilkes 2011).

The images of cotton fiber evolution in NaOH solution at 45 °C are shown in Fig. 2. Fibers show minor, intermediate, and swelling in a 5.5, 12, and 18 wt% NaOH-water solvents in the selected conditions 45 °C, respectively. The swelling behavior of cellulose fibers in the relatively low NaOH solution indicates the weak solvating power. When the cotton fibers are steeped in 12, and 18 wt% NaOH solution, cotton fibers lose crystalline structure observed by the intermediate swelling and swelling phenomenon within 10 min. The fiber swelling ratio kept constant

**Fig. 2** Optical microscopy images of cotton at 45 °C in 5.5, 12, 18 wt% NaOH solution



after 10 min (Fig. 3). The morphological changes of the cotton fibers at 45 °C are slightly higher than that at 36 °C, swelling ratios 1.5:1.4, 2:1.7, 2.3:2 at 5.5, 12, and 18wt % concentrations, respectively. In general, no ballooning phenomenon can be observed in the single cotton fiber steeping trials. Cuissinat and Navard (2006) reported that plant cell wall structures limit the swelling in cotton (and DWP) instead of fringed-fibrillar and semi-crystalline sub-structures. Their previous studies observed ballooning using NMMO with 25 to 35% water-treated cotton at around 90 °C.

#### Dissolving wood pulp

Figure 4 presents the morphological changes of DWP fibers in 5.5, 12, and 18 wt% NaOH solutions at 36 °C. We observed a pronounced increase in the fiber width, and the inner layer of the fiber has been disintegrated at 12 wt% solution. DWP fibers steeped in both 5.5 and 18 wt% solutions showed similar swelling behavior. At 20 °C and 36 °C (Fig. 5), fiber swells more in 12 wt% NaOH solution in such relatively low reaction temperatures, which had been confirmed in previous studies (Wilkes 2011). This effect reflected that both NaOH concentration and treatment temperature govern the solvating power of NaOH-water solution. An increase in the temperature associated with too high or too low NaOH concentration decreases the solvating influence of the NaOH solvent (Le Moigne 2008).

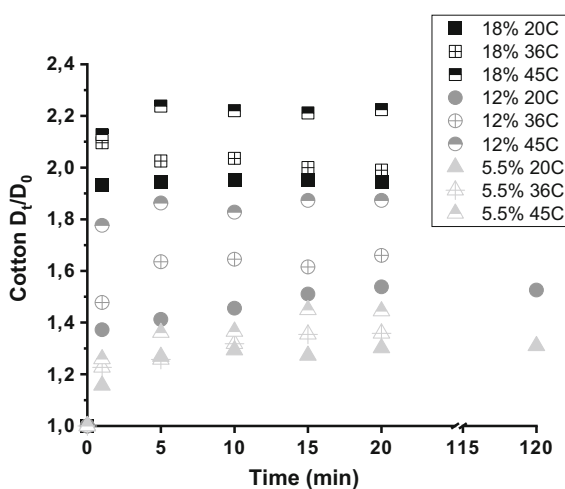


**Fig. 3** Evolution of cotton normalized width as a function of time

On the other hand, fiber swelling is mainly explained by the progressive attack of solvent in amorphous areas and H-bond interactions with the hydroxyl groups in these regions, which are better accessible than those in crystalline regions (Rosenau et al. 2019). At higher temperatures (45 °C), the NaOH-water solution dissolves more of the short-chain material. Some depolymerization also takes place during steeping, and the extent of depolymerization will increase with the increasing temperature that eventually leads to partial dissolution of the pulp (Mozdyniewicz et al. 2013). This could be explained by the low DP of DWP, which can be nearly fully dissolved, with few insoluble particles present. The swelling in these trials is much less dramatic than the previous studies, i.e., Cuissinat and Navard (2006) and Le Moigne et al. (2010), owing to the difference in the experimental conditions. Their studies used 8 wt% NaOH treated wood fiber at  $-10$  °C and  $-5$  °C. Furthermore, the cellulose fiber with larger DP with their original structure were put in contact with low NaOH concentration solution, which led to the mode 3 behavior where the fiber swells by ballooning but without dissolution. (Cuissinat and Navard 2006).

In the industrial scale viscose process, bleached dissolving wood pulp is typically the raw material and treated with steeping lye, containing a NaOH concentration of about 18 wt%. A higher NaOH solution was used to achieve optimal alkali cellulose quality. In this step and subsequent pre-aging, cellulose is converted into alkali cellulose for xanthation, and its degree of polymerization is adjusted to a level required for further processing. In these studies, we suggest applying steeping temperature of 45 °C, which was similar reported (a temperature of around 50 °C) by Mozdyniewicz et al. (2013). Furthermore, the formation of the raw material also influences the swelling behavior. In the case of DWP, pulp sheet may be used instead of powders for steeping. The highly compact structure and low surface area of the pulp sheet seriously lower the swelling rate of the cellulose. As for the raw material with a long fiber format, the surface area has to be reduced by employing grinding to improve the penetration of the liquor into materials. Grinding is also essential to avoid accumulating the fibers on the impeller, which may lead to non-homogenous lye.

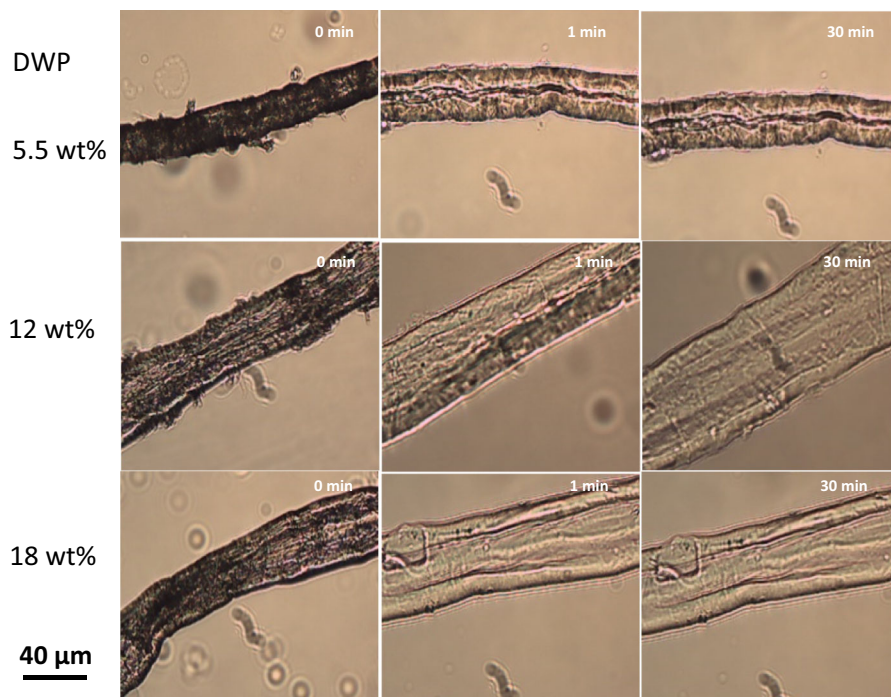


**Fig. 4** Optical microscopy images of DWP at 36 °C in 5.5, 12, 18 wt% NaOH solution

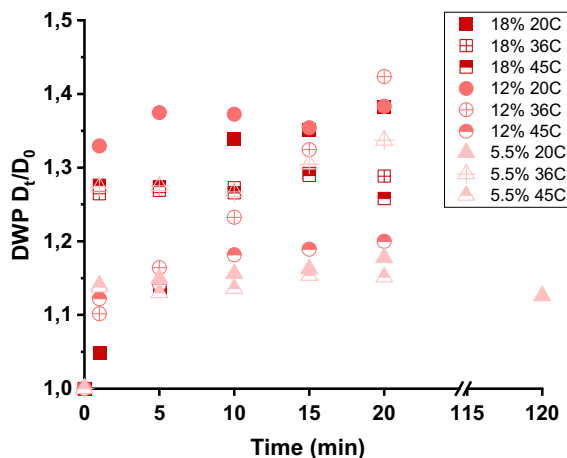


**Fig. 5** Evolution of DWP normalized width as a function of time

#### Viscose staple fiber and Tencel staple fiber

Alkali treatment transforms the structure of native cellulose I of DWP and cotton into cellulose II. This transformation is generally known as mercerization. For regenerated fibers composed of cellulose II, the alkali treatment only increases the amorphous phase of the fibers (Rojo et al. 2013). The fibers' swelling

behavior upon the solvents' addition at different temperatures is presented in Figs. 6 and 7.

VsF and TsF fiber swell more in 12 wt% NaOH solution (Figs. 6 and 7), similar to DWP swelling; those fibers' swelling increases as the concentration is reduced. These conditions increase the amorphous regions of the fibers and swell the microfibrils and fibers. The normalized width  $D_t/D_0$  of fibers placed in NaOH is plotted in Fig. 8 a,b as a function of time. VsF was swelling severely at 45 °C. In contrast, TsF was swelling severely at 20 °C. No ballooning or splitting tendency of TsF was observed irrespective of whether the fiber ends were fixed or free. Öztürk et al. series studies (2006a, b 2009) reported that depending on shear force, alkali concentration (up to 5 M), and alkali type, different splitting of fiber into 15–40 fibrils were observed. Above 5 M, cation type of alkali is no more relevant to splitting lyocell fiber, due to the homogeneous distribution of alkali occurs, resulting in a decrease in swelling stress. Chaudemanche and Navard (2011) showed that lyocell fibers are swelling as a typical polymer, i.e., inwards swelling of the fiber. Whereas in actual swelling, the hollow DWP fibers can swell both outwards and inwards. This has profound consequences on the way of dissolving



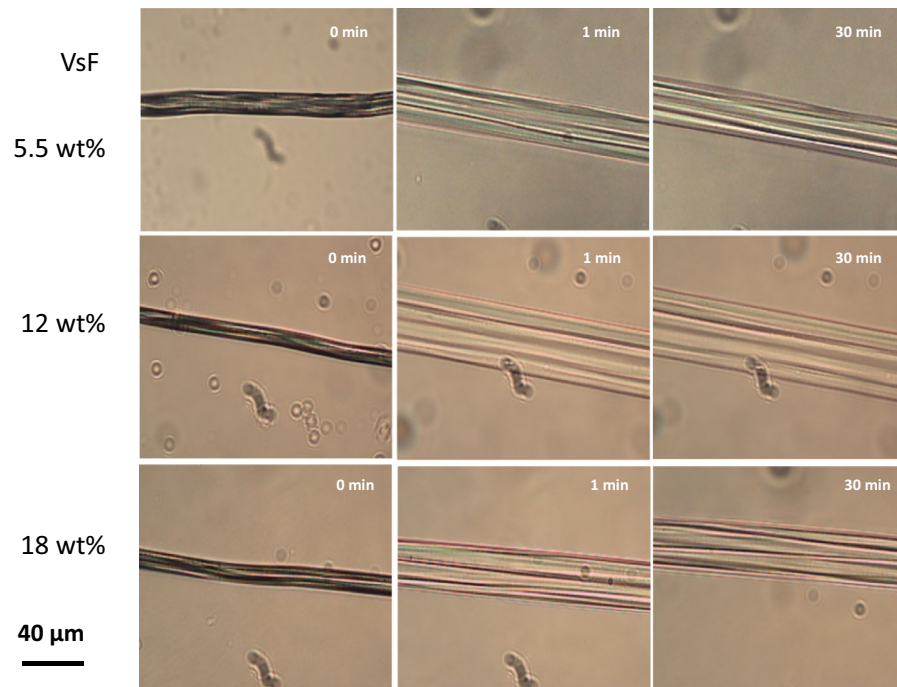


**Fig. 6** Optical microscopy images of VsF at 45 °C in 5.5, 12, 18 wt% NaOH solution

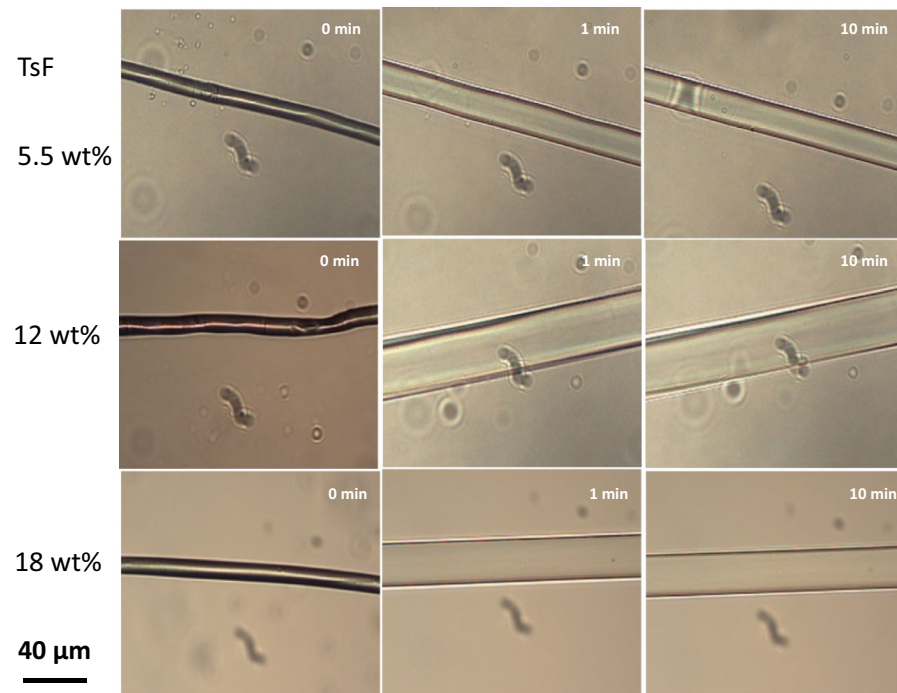


**Fig. 7** Optical microscopy images of TsF at 20 °C in 5.5, 12, 18 wt% NaOH solution

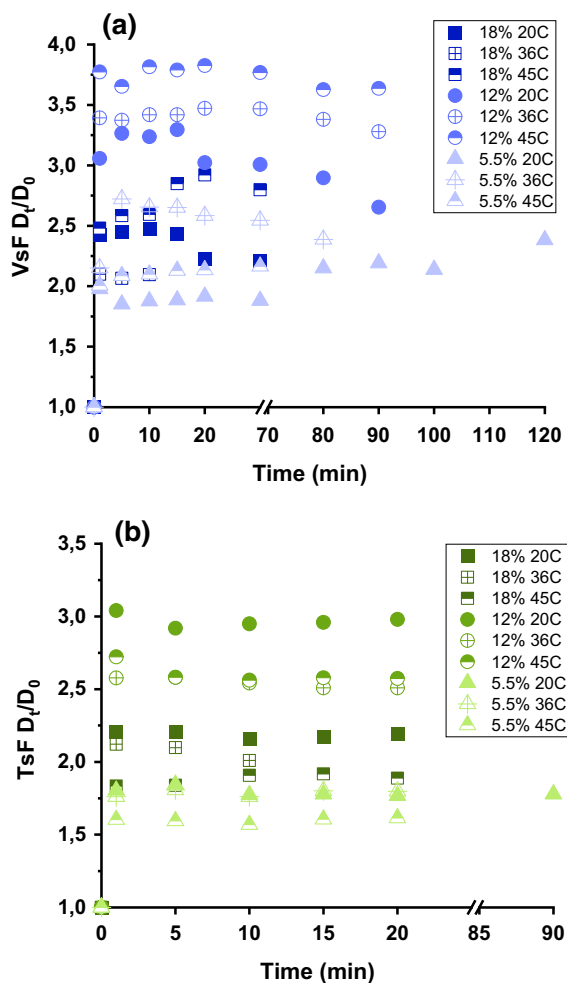


**Fig. 8** Evolution of (a) VsF, and (b) TsF normalized width as a function of time

nature and regenerated fibers. For the regenerated cellulosic textile fibers, VsF and TsF, such structures also formed during the biosynthesis (i.e., wet-spinning) of plant cell walls, resulting in cellulose molecules' inherent tendency. However, also other factors like hornification of fibers during drying may limit swelling.

## Conclusions

The swelling behaviors of the selected fibers highly rely on the treatment conditions and the physical and chemical properties of the raw materials. Depending on NaOH concentrations and reaction time, minor swelling, intermediate swelling, and complete

swelling of cotton, DWP, viscose, and Tencel fibers were observed. Increasing the temperature and/or NaOH content improves the more considerable swelling of cotton and DWP fibers. The applicability of the cotton should be used for alkaline steeping at higher temperatures as used during the viscose process. When considering utilizing VsF and TsF in alkali steeping, at relatively lower lye concentration, i.e., 12 wt% and temperatures, i.e., 20 °C, are suggested.

**Acknowledgments** The financial support from Jenny and Antti Wihuri Foundation (Grant No. 131219) is gratefully acknowledged. The authors wish to thank Maija Nenonen and Sari Larmu for simulating the industrial viscose process. We thank Dr. Daisuke Sawada (Aalto University) for the crystallinity calculation. Additionally, the authors acknowledge the provision of the facility and technical support by Aalto University at OtaNano-Nanomicroscopy Center (Aalto NMC).

**Authors' contributions** Dr. Xiang You was responsible for the experimental design with Dr. Feng Chen and Dr. Annariikka Roslli, performed the experimental work, analyzed the corresponding results, and wrote the manuscript as principal author, with copyediting by Dr. Feng Chen, Dr. Yibo Ma, and Dr. Heikki Hassi, under the supervision of Dr. Eric Enqvist and Dr. Heikki Hassi.

**Funding** The financial support was from Jenny and Antti Wihuri Foundation (Grant No. 131219).

**Data availability** The authors declare that the data and material are available.

## Declarations

**Conflicts of interest** The authors declare that they have no conflict of interest.

**Consent to participate** The authors declare that they agree to participate.

**Consent to publication** The authors declare that they agree to publication.

## References

- Abu-Rous M, Ingolic E, Schuster KC (2006) Visualisation of the fibrillar and pore morphology of cellulosic fibres applying transmission electron microscopy. *Cellulose* 13:411–419. <https://doi.org/10.1007/s10570-006-9052-5>
- Abu-Rous M, Varga K, Bechtold T, Schuster KC (2007) A new method to visualize and characterize the pore structure of

- TENCEL (Lyocell) and other man-made cellulosic fibres using a fluorescent dye molecular probe. *J Appl Polym Sci* 106:2083–2091. <https://doi.org/10.1002/app.26722>
- Chaudemanche C, Navard P (2011) Swelling and dissolution mechanisms of regenerated Lyocell cellulose fibers. *Cellulose* 18:1–15. <https://doi.org/10.1007/s10570-010-9460-4>
- Chen F, Sawada D, Hummel M, Sixta H, Budtova T (2020) Swelling and dissolution kinetics of natural and man-made cellulose fibres in solvent power tuned ionic liquid. *Cellulose* 27:7399–7415. <https://doi.org/10.1007/s10570-020-03312-5>
- Cuissinat C, Navard P (2006) Swelling and dissolution of cellulose part II: free floating cotton and wood fibres in NaOH-water-additives systems. *Macromol Symp* 244:19–30. <https://doi.org/10.1002/masy.200651202>
- Cuissinat C, Navard P (2008) Swelling and dissolution of cellulose, Part III: plant fibres in aqueous system. *Cellulose* 15:67–74. <https://doi.org/10.1007/s10570-007-9158-4>
- Deslauriers M, Trozzi C, Woodfield M (2006) Processes in wood, paper pulp, food, drink and other industries - Paper pulp (acid sulphite process). In: EMEP/CORINAIR Emission Inventory Guidebook. SNAP code 040603, Chapter B463, European Environment, pp 1–12
- Dochia M, Roskwitalski Z (2012) Cotton fibres. In: Kozłowski RM (ed) Handbook of natural fibres, vol 1. Woodhead Publishing, Cambridge, UK, pp 11–23
- Foress KG, Fremer KE (2003) The nature and reactions of lignin - a new paradigm. Oy Nord Print Ab, Helsinki, p 128
- Gross AS, Chu JW (2010) On the molecular origins of biomass recalcitrance: the interaction network and solvation structures of cellulose microfibrils. *J Phys Chem B* 114:13333–13341. <https://doi.org/10.1021/jp106452m>
- Guizani C, Larkiala S, Moriam K, Sawada D, Elsayed S, Rantasalo S, Sixta H (2020) Air gap spinning of a cellulose solution in [DBNH][OAc] ionic liquid with a novel vertically arranged spinning bath to simulate a closed loop operation in the Ioncell process. *J Appl Polym Sci* 138:49787. <https://doi.org/10.1002/app.49787>
- Heinze T, Koschella A (2005) Solvents applied in the field of cellulose chemistry- a mini review. *Polimeros* 15:84–90. <https://doi.org/10.1590/S0104-14282005000200005>
- Henniges U, Kostic M, Borgards A, Rosenau T, Potthast A (2011) Dissolution behavior of different celluloses. *Biomacromol* 12:871–879. <https://doi.org/10.1021/bm101555q>
- Kihlman M, Aldaeus F, Chedid F, Germgård U (2012) Effect of various pulp properties on the solubility of cellulose in sodium hydroxide solutions. *Holzforschung* 66:601–606. <https://doi.org/10.1515/hf-2011-0220>
- Kihlman M, Medronho B, Romano A, Germgård U, Lindman B (2013) Cellulose dissolution in an alkali based solvent: Influence of additives and pretreatments. *J Braz Chem Soc* 24:295–303. <https://doi.org/10.5935/0103-5053.20130038>
- Kleman-Leyer K, Agosin E, Conner AH, Kirk TK (1992) Changes in molecular size distribution of cellulose during attack by white rot and brown rot fungi. *Appl Environ Microbiol* 58:1266–1270. <https://doi.org/10.1128/aem.58.4.1266-1270.1992>
- Klemm D, Heublein B, Fink HP, Bohn A (2005) Cellulose: fascinating biopolymer and sustainable raw material. *Angew Chem Int Ed* 44:3358–3393. <https://doi.org/10.1002/anie.200460587>
- Kreze T, Malej S (2003) Structural characteristics of new and conventional regenerated cellulosic fibres. *Text Res J* 73:675–684. <https://doi.org/10.1177/004051750307300804>
- Le Moigne N, Jardeby K, Navard P (2010) Structural changes and alkaline solubility of wood cellulose fibres after enzymatic peeling treatment. *Carbohydr Polym* 79:325–332. <https://doi.org/10.1016/j.carbpol.2009.08.009>
- Le Moigne N (2008) Swelling and dissolution mechanisms of cellulose fibres. Doctoral dissertation, École Nationale Supérieure des Mines de Paris, pp 9–32
- Liebert T (2010) Cellulose solvents- remarkable history, bright future. Cellulose solvents: for analysis, shaping and chemical modification. Publisher: Am Chem Soc Washington DC, pp 3–54. <https://doi.org/10.1021/bk-2010-1033.ch001>
- Mäkelä V, Wahlström R, Holopainen-Mantila U, Kilpeläinen I, King A (2018) Clustered single cellulosic fibre dissolution kinetics and mechanisms through optical microscopy under limited dissolving conditions. *Biomacromol* 19:1635–1645. <https://doi.org/10.1021/acs.biomac.7b01797>
- Moryganov AP, Zavadskii AE, Stokozenko VG (2018) Special features of X-ray analysis of cellulose crystallinity and content in flax fibres. *Fibre Chem* 49:382–387. <https://doi.org/10.1007/s10692-018-9904-4>
- Mozdyniewicz DJ, Nieminen K, Sixta H (2013) Alkaline steeping of dissolving pulp. Part i: Cell Degradation Kinetics Cell 20:1437–1451. <https://doi.org/10.1007/s10570-013-9926-2>
- Nishiyama Y, Langan P, Chanzy H (2002) Crystal structure and hydrogen-bonding system in cellulose I $\beta$  from synchrotron X-ray and neutron fibre diffraction. *Am Chem Soc* 124:9074–9082. <https://doi.org/10.1021/ja0257319>
- Nishiyama Y, Sugiyama J, Chanzy H, Langan P (2003) Crystal structure and hydrogen bonding system in cellulose I $\alpha$  from synchrotron X-ray and neutron fibre diffraction. *Am Chem Soc* 125:14300–14306. <https://doi.org/10.1021/ja0257319>
- O’Sullivan AC (1997) Cellulose: the structure slowly unravels. *Cellulose* 4:173–207. <https://doi.org/10.1023/A:1018431705579>
- Okubayashi S, Griesser UJ, Bechtold T (2004) A kinetic study of moisture sorption and desorption on lyocell fibers. *Carbohydr Polym* 58:293–299. <https://doi.org/10.1016/j.carbpol.2004.07.004>
- Okubayashi S, Griesser UJ, Bechtold T (2005) Water accessibilities of man-made cellulosic fibers—effects of fiber characteristics. *Cellulose* 12:403–410. <https://doi.org/10.1007/s10570-005-2179-y>
- Olsson C, Idström A, Nordstierna L, Westman G (2014) Influence of water on swelling and dissolution of cellulose in 1-ethyl-3-methylimidazolium acetate. *Carbohydr Polym* 99:438–446. <https://doi.org/10.1016/j.carbpol.2013.08.042>
- Olsson C, Westman G (2013) Direct dissolution of cellulose: background, means and applications. Cellulose - fundamental aspects. Publisher: InTech, Rijeka, pp 143–178. <https://doi.org/10.5772/52144>

- Öztürk HB, Okubayashi S, Bechtold T (2006a) Splitting tendency of cellulose fibers – Part 1. The effect of shear force on mechanical stability of swollen lyocell fibers. *Cellulose* 13:393–402. <https://doi.org/10.1007/s10570-006-9053-4>
- Öztürk HB, Okubayashi S, Bechtold T (2006b) Splitting tendency of cellulose fibers – Part 2: effect of fiber swelling in alkali solutions. *Cellulose* 13:403–409. <https://doi.org/10.1007/s10570-006-9054-3>
- Öztürk HB, Potthast A, Rosenau T, Abu-Rous M, MacNaughtan B, Schuster KC, Mitchell JR, Bechtold T (2009) Changes in the intra- and inter-fibrillar structure of lyocell (TEN-CEL®) fibers caused by NaOH treatment. *Cellulose* 16:37–52. <https://doi.org/10.1007/s10570-008-9249-x>
- Palme A, Idström A, Nordstierna L, Brelid H (2014) Chemical and ultrastructural changes in cotton cellulose induced by laundering and textile use. *Cellulose* 21:4681–4691. <https://doi.org/10.1007/s10570-014-0434-9>
- Placet V, Trivaudey F, Cisse O, Gucheret-Retel V, Boubakar ML (2012) Diameter dependence of the apparent tensile modulus of hemp fibres: a morphological, structural or ultrastructural effect? *Compos Part A Appl Sci Manuf* 43:275–287. <https://doi.org/10.1016/j.compositesa.2011.10.019>
- Rojo E, Virginia Alonso M, Domínguez JC, Saz-Orozco BD, Olier M, Rodríguez F (2013) Alkali treatment of viscose cellulosic fibres from eucalyptus wood: Structural, morphological, and thermal analysis. *J Appl Polym Sci* 130:2198–2204. <https://doi.org/10.1002/app.39399>
- Rosenau T, Potthast A, Hofinger A, Bacher M, Yoneda Y, Mereiter K, Nakatsubo F, Jäger C, French AD, Kajiwaru K (2019) Toward a better understanding of cellulose swelling, dissolution, and regeneration on the molecular level. In: Rosenau T, Potthast A, Hell J (eds) *Cellulose science and Technology chemistry, analysis and application U. Natural Resources and Life Sciences*, Vienna (BOKU), pp 99–120
- Schelosky N, Röder T, Baldinger T, Milacher W, Morgenstern B, Sixta H (1999) Molecular mass distribution of cellulosic products by size exclusion chromatography in DMAc/LiCl. *Das Papier* 12:728–738
- Schuster KC, Aldred P, Villa M, Baron M, Loidl R, Biganska O, Patlazhan S, Vavard P, Rüd H, Jericha E (2003) Characterising the emerging Lyocell fibres structures by ultra small angle neutron scattering (USANS). *Lenzinger Berichte* 82:107–117
- Sen S, Martin J, Argyropoulos D (2013) Review of cellulose non-derivatizing solvent interactions with emphasis on activity in inorganic molten salt hydrates. *ACS Sustain Chem Eng* 1:858–870. <https://doi.org/10.1021/sc400085a>
- Siroka B, Noisternig M, Griesser UJ, Bechtold T (2008) Characterization of cellulosic fibers and fabrics by sorption/desorption. *Carbohydr Res* 343:2194–2199. <https://doi.org/10.1016/j.carres.2008.01.037>
- Sixta H (2006) Chemical pulping process: sections 4.2.8–4.3.6.5. *Handbook of Pulp*. Wiley-VCH Verlag GmbH, Weinheim, Germany, pp 366–509
- Timpa JD, Ramey HH (1989) Molecular characterization of three cotton varieties. *Text Res J* 59:661–664. <https://doi.org/10.1177/004051758905901105>
- Wilkes A (2011) The viscose process. In: Woodings C (ed) *Regenerated cellulose fibres*, vol 1. The Textile Institute. Woodhead Publishing Limited, Cambridge, pp 37–61
- Xie Y, Hill CA, Jalaludin Z, Curling SF, Anandjiwala RD, Norton AJ, Newman G (2011) The dynamic water vapour sorption behaviour of natural fibres and kinetic analysis using the parallel exponential kinetics model. *J Mater Sci* 46:479–489. <https://doi.org/10.1007/s10853-010-4935-0>
- Zhang S, Wang W, Li F, Yu J (2013) Swelling and dissolution of cellulose in NaOH aqueous solvent systems. *Cellul Chem Technol* 47:671–679

**Publisher's Note** Springer Nature remains neutral with regard to jurisdictional claims in published maps and institutional affiliations.